Novel signatures for long-lived particles at the LHC

Shankha Banerjee,[1,*] Geneviève Bélanger,[1,†] Biplob Bhattacherjee,[2,‡]
Fawzi Boudjema,[1,§] Rohini M. Godbole,[2,¶] and Swagata Mukherjee[3,**]

[1] *LAPTh, Université Savoie Mont Blanc, CNRS, B.P. 110, F-74941 Annecy, France*
[2] *Centre for High Energy Physics, Indian Institute of Science, Bangalore 560012, India*
[3] *III. Physikalisches Institut A, RWTH Aachen University, Otto-Blumenthal-Str. 16, 52074 Aachen, Germany*

(Dated: June 23, 2017)

In the context of searches for long-lived particles (LLP), we have shown, using several benchmarks, that objects which emerge from a secondary vertex due to the decay of an LLP at the TeV scale, are often at large angular separations with respect to the direction of the parent LLP and a fraction of the decay products can even go in the backward direction. These will give rise to striking signatures in the detectors at the LHC. It is worthwhile to perform dedicated searches for these signatures, and we suggest some variables that could be used to identify such unconventional signatures and reduce backgrounds coming from instrumental noise and cosmic rays.

Long-lived massive particles (LLP) are predicted in whole classes of extensions of the standard model (SM) that are motivated by either the hierarchy problem [1, 2], naturalness [3, 4], dark matter (DM) [5] or the baryon-antibaryon asymmetry in the universe [6]. Massive particles with lifetimes between 100 picoseconds and a few nanoseconds lead to very peculiar signatures at colliders as they decay some distance (tens to hundreds of centimeters) from the interaction point. Dedicated searches for these new particles through their exotic signatures are being pursued actively by the ATLAS, CMS and LHCb Collaborations at the Large Hadron Collider (LHC). Long-lived neutral particles will lead to signatures which include displaced vertices with jets or leptons [7–11], lepton jets (collimated jets of light leptons and hadrons) [12–14], emerging jets [15] or non-pointing objects [16]. Long-lived charged particles decaying in the detector will lead to disappearing tracks [17] or tracks with kinks [18–20]. Displaced vertices in exotic Higgs decays into LLPs also provide distinctive signatures [21–24]. Moreover, specific searches are also designed to look for particles that lose all their energy and decay after coming to rest within the detector [25–27].

Several searches have concentrated on charged particles that are long-lived enough to escape the detector. These searches at the LHC focus on the measurements of the energy loss dE/dx due to ionisation in the tracker and on the measurement of the time-of-flight (TOF) of the LLP to the outer detectors like the muon chamber [28, 29].

Generically, in standard model extensions, a few mechanisms are responsible for the long lifetime of a new particle. A small mass splitting (for example in the case of a chargino almost degenerate with a neutralino LSP in AMSB models [30]), a suppression due to the high mass of the propagator (for example with R-hadrons as bound states of gluino ($\tilde{g}$) in split SUSY scenarios with very heavy squarks [31, 32]) or a suppressed coupling can all lead to lifetimes exceeding ~ 100 picoseconds. The suppressed coupling scenario can be found for example in SUSY models with a gravitino LSP (lightest supersymmetric particle) [18, 19, 33], in scenarios with violation of R-parity(RPV) [34, 35], or generically in models containing a hidden sector that is weakly coupled to the SM via some mediator as in Hidden valley models [36, 37]. LLPs also arise naturally in dark matter models, in particular in those models which do not rely on the standard freeze-out mechanism. For example in models featuring very weakly interacting particles that rely on the freeze-in mechanism, a new particle that decays into dark matter will be an LLP [5, 35, 38]. LLPs are also found in models with asymmetric DM where the dark sector contains dark baryons and mesons at the TeV scale that decay into SM with a slow decay rate [39].

When an LLP is produced at the primary vertex and decays somewhere inside the detector after traversing a certain distance, *i.e.*, at the secondary vertex, a typical search method is to identify this displaced vertex. However, if the produced LLP is slow (typically heavy particles with mass $\mathcal{O}$(TeV) have this feature), then in addition to the displaced vertex, there can be other unique features of the decay products. This forms the main motivation for our work. Before getting into the details of these special features for an LLP, let us discuss the general properties of the decay products ensuing from any heavy particle.

Let us consider production of a pair of heavy particles denoted by X, for example squarks or gluinos in supersymmetric models. It is interesting to see the alignment of the daughter particles with respect to the original direction of the parent particle in this case. To illustrate this we consider four distinct possibilities, a) $X \to q\ q\ q$, b) $X \to q\ q$, c) $X \to q\ q$ DM and d) $X \to q$ DM, where q denotes a *massless* quark and DM signifies a heavy

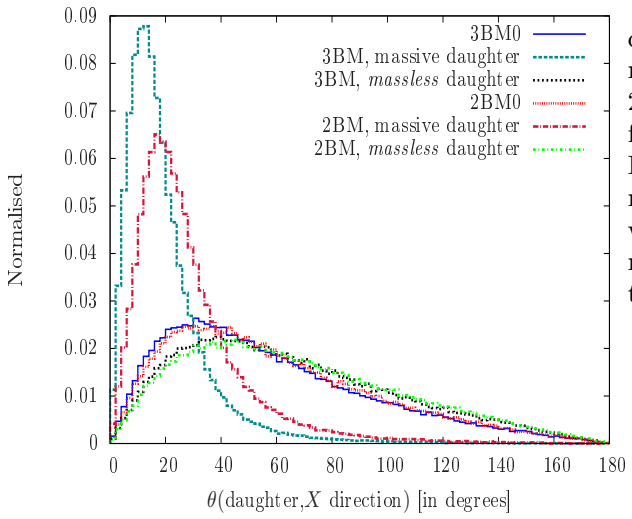

FIG. 1. Angle θ made by a daughter particle with the direction of X for $M_X = 2$ TeV for 3BM0 (blue solid), 3BM massive (dark cyan dashed), 3BM massless (black dotted), 2BM0 (red fine dotted), 2BM massive (crimson dot-dashed) and 2BM massless (lime fine dot-dashed).

invisible particle which may satisfy the properties of dark matter. Examples of the former two signatures with *massless* decay products can come about from R-parity violating decays of a gluino ($\tilde{g} \to q\ q\ q$) or from a squark ($\tilde{q} \to q\ q$), giving rise to a multiple jets final state. The latter two signatures can be illustrated in terms of R-parity conserving SUSY, *viz.*, $\tilde{g} \to q\bar{q}\chi_1^0$ and $\tilde{g} \to g\chi_1^0$, where χ_1^0 is the massive LSP and may serve as a dark matter candidate. These give rise to the final states of multiple jets and missing transverse energy (MET). We denote these aforementioned cases as follows: two-body (three-body) decays involving all *massless* decay products as 2BM0 (3BM0) and similar decays with one massive invisible daughter as 2BM (3BM).

Case	M_X [TeV]	β (mean, RMS)	$\theta > 22.5^\circ$	$\theta > 45^\circ$	$\theta > 90^\circ$	$\theta > 135^\circ$
2BM0	0.2	0.87, 0.13	0.78	0.46	0.13	0.03
	0.5	0.81, 0.14	0.94	0.65	0.19	0.04
	1	0.72, 0.15	0.99	0.83	0.28	0.06
	3	0.49, 0.12	1.00	1.00	0.50	0.11
2BM	0.2	0.74, 0.21	0.67	0.40	0.13	0.03
	0.5	0.66, 0.21	0.77	0.50	0.17	0.04
	1	0.57, 0.19	0.84	0.58	0.21	0.05
	3	0.38, 0.14	0.91	0.72	0.31	0.07
3BM0	0.2	0.94, 0.09	0.65	0.34	0.09	0.02
	0.5	0.86, 0.13	0.92	0.61	0.20	0.04
	1	0.76, 0.15	0.99	0.84	0.33	0.07
	3	0.50, 0.13	1.00	1.00	0.65	0.16
3BM	0.2	0.77, 0.19	0.84	0.58	0.22	0.05
	0.5	0.69, 0.19	0.92	0.70	0.28	0.06
	1	0.61, 0.18	0.96	0.79	0.35	0.08
	3	0.40, 0.14	0.99	0.91	0.51	0.13

TABLE I. Mean value and dispersion (rms) of the velocity of the daughter particle and fraction of events with angle θ made by at least one of the lightest daughter particles with the direction of X for the four scenarios, *viz.*, 2BM0, 2BM, 3BM0 and 3BM respectively. For the massive scenarios, $M_{\rm DM} = 0.75 \times M_X$.

In the following, we generate the above four cases at parton level for the 14 TeV LHC scenario using `PYTHIA 6` [40]. The 2BM0 (3BM0) and 2BM (3BM) scenarios are respectively generated for quark initiated and gluon initiated processes. In figure 1 we show the angle the *massless* and massive decay particles ($M_{\rm DM} = 0.75 \times M_X$) make with the direction of motion of X for a benchmark mass of $M_X = 2$ TeV. From this figure, we gather that

- The massless particles emanating from X need not be aligned along the initial direction of X. The massive daughter particle, however, is less boosted and therefore more aligned with the initial direction of X.
- The fraction of *massless* particles having large angles with respect to the direction of X, can be significant. We even find that a substantial fraction of *massless* daughter particles move in a backward direction, *i.e*, at angles 90° or more with respect to the initial direction of X.
- It is also seen that upon having a heavy invisible particle in the decay spectrum, in scenarios 3BM and 2BM, the *massless* daughter tends to be further separated from the direction of X compared to the corresponding all-*massless* scenario, 3BM0 and 2BM0. We can see that the peak of the black dotted (lime fine dot-dashed) curve is shifted to the right of the blue solid (red fine dotted) curve.

In table I, we estimate the fraction of instances when at least one *massless* decay particle [1] makes a certain angle ($\theta > 22.5^\circ$, $\theta > 45^\circ$, $\theta > 90^\circ$ or $\theta > 135^\circ$) with respect to the direction of X for $M_X = 200$ GeV, 500 GeV, 1 TeV, and 3 TeV. For illustration, we choose the heavy invisible daughter particle mass to be $M_{\rm DM} = 0.75 \times M_X$. The quantity β denotes the velocity of X. Note that as expected and for a fixed mass, quark initiated processes (2BM0 and 3BM0) have a larger β than gluon initiated processes (2BM and 3BM). Moreover in a given scenario as β decreases there is a larger fraction of the daughter particles found at large angles [2]. We also find that at least one *massless* daughter particle can be separated from the

[1] Because the samples have been generated for SUSY processes using `PYTHIA 6`, there is no spin information and hence for the full *massless* scenario, the angular distribution for all the daughter particles are identical.

[2] Since we are considering the particle motion in the transverse direction, the velocity in the transverse direction, β_T is a more pertinent quantity. We found that the mean and rms values of β_T do not vary significantly with

direction of X by 90 degrees or more for $\mathcal{O}(20\ \%)$ cases for M_X as low as 500 GeV.

Although, such angular distributions are well-known, their implications for LLP searches have not yet been investigated in details. An LLP, upon production, moves a certain distance inside the detector and decays in some of the aforementioned ways. Following the previous discussion, we find that most of the *massless* decay products will not follow the original direction of the LLP and a substantial fraction of these particles may even move in the backward direction with respect to the LLP direction. Here, we must make the important distinction between daughter particles moving in the backward direction when they are produced at the primary vertex or at the secondary vertex. When the decay occurs basically at the interaction point, a particle is always travelling in the outward direction, whereas a particle moving backwards having been generated at a secondary vertex has a whole new meaning. Depending on the angular separation of the *massless* daughter with respect to the direction of the LLP, as shown in figure 1, we can have two distinct experimental signatures, *viz.*,

- ***Distorted objects:*** Jets ensuing from the primary vertex, termed as prompt jets, will have a circular deposition of energy in the $\eta - \phi$ plane of the calorimeters. In spite of the non-pointing geometry of the calorimeters, such jets, in most cases, are contained inside a single tower of HCAL. This is shown in the left column in the schematic diagram 2. On the contrary, jets emanating from a secondary vertex, displaced with respect to the point of collision, termed as non-prompt jets, will pass through multiple calorimeter towers yielding elliptical energy deposition in the $\eta - \phi$ plane, as seen in the right column of diagram 2. Similar energy distributions in the ECAL are expected from prompt and non-prompt photons as shown in Ref. [41]. The distortion will depend on the angle the daughter makes with the direction of the LLP as well as the on its displacement from the primary vertex before it decays. This distortion will be more prominent for boosted objects like top, $W/Z/H$ jets. We classify these as *distorted objects (DOs)*. Dedicated experimental input is required to realistically simulate the effect of this distortion.

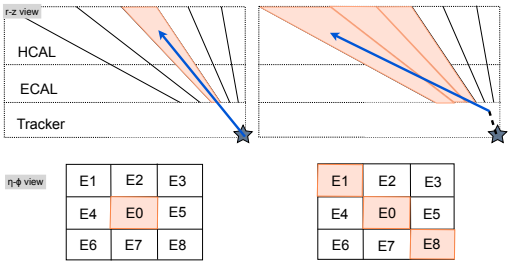

FIG. 2. Simplified diagram showing signature of prompt and displaced jets in calorimeters

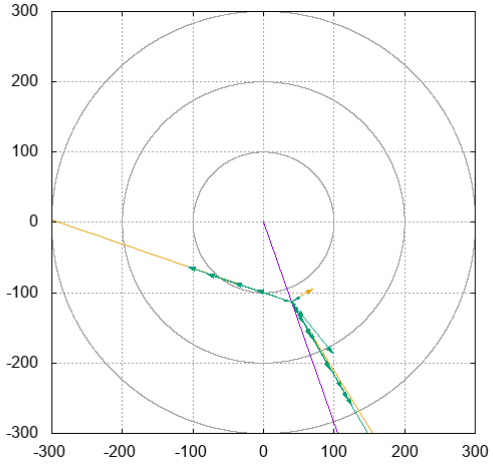

FIG. 3. Representative decays of an LLP in the xy (transverse)plane.

- ***Backward moving objects:*** If the separation angle is sufficiently large, the daughter particle(s) will move in the backward direction and can even cross inward layers of the detector. We term such particles as *backward moving objects (BMOs)*. To the best of our knowledge, dedicated searches for such objects are yet to be performed at the LHC. In this work, we emphasize the significance of such searches and construct a few possible observables to look for such signatures.

For example, if an LLP decays in the ECAL, the *BMOs* will tend to move towards the tracker [3]. We elucidate this point with a typical event display in the xy-plane (see figure 3) where an LLP (purple vector) is produced and decays to three quarks (yellow vectors) after having travelled a certain distance in the detector. We indeed find

the LLP mass. However we computed the third moment (skewness) and the fourth moment (kurtosis) and found that because these distributions are asymmetric, the kurtosis parameter play a significant role in discriminating the β_T distributions, increasing with the mass.

[3] This statement can be generalised in the context of decay products of an LLP moving from any outward detector segment to an inner one, for example an LLP decaying inside the muon chamber and the daughter particles moving into the HCAL.

that the hadronised stable particles (green vectors) have angular separations with respect to the LLP direction, some being classified as *DOs* and some as *BMOs*.

In order to quantify the energy carried by the *BMOs*, we resort to a simple minded geometrical analysis. We approximately follow the dimensions of the CMS detector [42] to quantify our analyses. However, the results can be generalised for any general purpose detector with similar dimensions, for instance ATLAS. We consider the tracker as an open cylinder having a length $L_{\rm tracker} = 600$ cm along the z-direction and a radius $R_{\rm tracker} = 100$ cm. The last layer of the HCAL is considered to be at a transverse distance of 300 cm from the z-axis. For simplicity, we only consider discussions pertaining to the barrel. The results can be extended by including end-caps to our geometry.

Having defined the geometry, we next compute the fraction of energy carried by particles moving in the backward direction and into the tracker volume. In order to do so, we employ a trivial geometry concerning a ray crossing a finite open cylinder. If the LLP decays between 100 cm and 300 cm in the transverse direction (*i.e.*, somewhere in between the tracker and the HCAL), we compute the ratio of energy carried by the *BMOs* and into the tracker volume, $E_{\rm in}$ to the initial energy carried by the LLP, $E_{\rm LLP}$. To simulate this, we pair produce LLPs and for simplicity, in our analyses, we focus on one such LLP per event. On the other hand, we also simulate a scenario where the LLPs come to a halt (stopped R-hadrons) between 100 cm and 300 cm in the transverse direction and decay. We boost back all the daughter particles of that particular LLP to the stopped R-hadron's rest frame and calculate the fraction of energy carried by the daughter particles traversing in the backward direction and inside the tracker. In figure 4, we illustrate the ratio of the energy carried by the visible daughter particles inside the tracker ($E_{\rm in}$) and the energy carried by the mother LLP ($E_{\rm LLP}$). We show our results for moving LLPs as well as for stopped R-hadrons. For all scenarios, we see that $E_{\rm in}/E_{\rm LLP}$ is larger for the stopped R-hadron case. This distinction is striking for the case when all the daughters are *massless*. For such scenarios, the fractions of energy coming back inside the tracker are respectively 12.2% (14.2%) and 25.9% (34.2%) for the moving LLP and the stopped R-hadron for a two-body (three-body) decay of the LLP. When one of the daughters is a massive invisible particle, the situation changes drastically. The heavy daughter moves forward mostly in the direction of the mother LLP (as shown in figure 1). The energy fractions traversing back into the tracker are respectively 5.1% (2.5%) and 8.2% (4.6%) for the moving LLP and the stopped R-hadron case for the two-body (three-body) decay of the LLP. Upon varying the mass of the heavy inviable daughter particle, we find that the fraction $E_{\rm in}/E_{\rm LLP}$ changes appreciably. As an example, for $M_{\rm LLP} = 2$ TeV, this fraction decreases approximately linearly from 8.5% to 5.1% upon changing $M_{\rm DM}/M_{\rm LLP}$ from 0% (for example a scenario involving a gravitino) to 75%. Even though the $E_{\rm in}$ fractions involving a massive scenario are smaller with respect to their *massless* counterparts, these numbers can be considered significant given the dearth of SM background events in the backward direction, produced at the LHC. The results presented above focused on a single LLP. However, daughter particles moving in the backward direction can occur from either of the pair produced LLPs, hence the number of such particles will be enhanced.

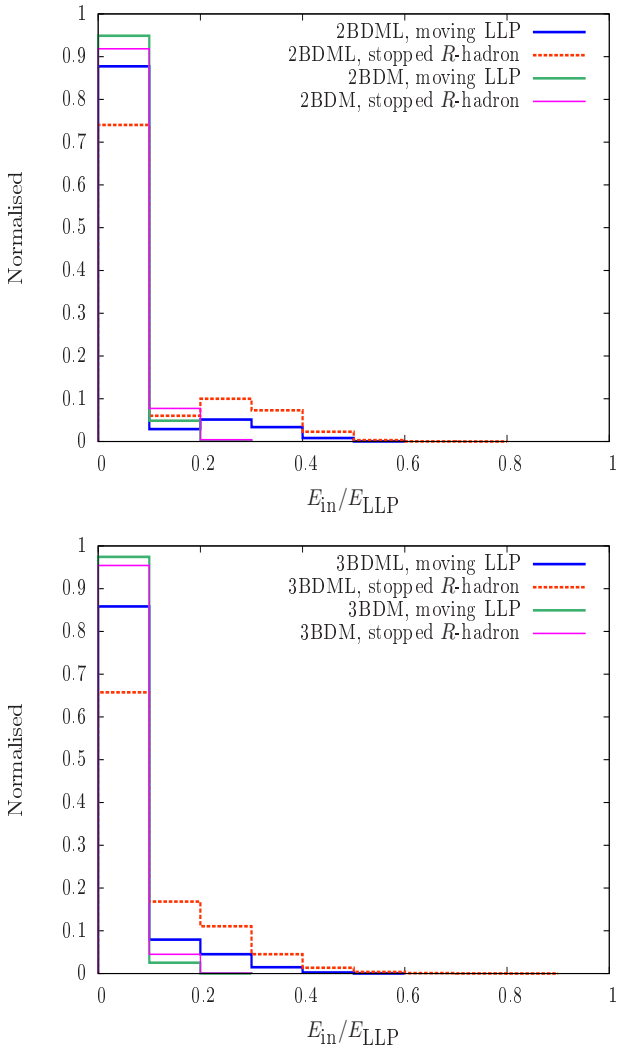

FIG. 4. Energy fraction of visible daughter particles to the mother LLP. $M_{\rm DM} = 0.75 \times M_{\rm LLP}$. $E_{\rm in} = 0$ for the first bin. Upper (lower) plots are for 2-body (3-body) LLP decays.

The *DO*s and *BMO*s, that are heavily displaced with respect to the primary vertex, having large impact parameters, are likely to be missed by the currently used jet reconstruction algorithms, because such algorithms are based on the assumption that the jets are originating from the collision point. However, the jet reconstruction algorithm can be tuned to catch displaced jets. This option can be heavily resource-consuming and the experiments can utilise the ideas of data-scouting and parking [43]. Reconstructing *DO*s or *BMO*s with large impact parameters in tracker can be extremely challenging. Even if it can be achieved by making modifications in track reconstruction algorithms, relaxing the requirement on the impact parameter of the track, it will be very difficult to distinguish between signal and background tracks. However, a recent study has shown the capabilities of the HL-LHC in extracting more information from non-pointing tracks [44].

A set of dedicated triggers might be needed to select such signal events with in LHC experiments. One possibility is to require multiple displaced jets with appropriate p_T cuts. Otherwise one can trigger on the sum of HCAL energy deposits.

Although the SM backgrounds are expected to be small for this kind of search, there can be challenges coming from instrumental noise, beam-induced noise, overwhelming number of overlapping events in LHC experiments and most importantly from cosmic ray events. However, one can exploit the striking signatures of the signal to reject backgrounds originating from the *pp* collisions. Shower-shape for an inside-out jet is expected to be different from a backward-moving outside-in jet. There are widely used shower-shape variables for the ECAL, *viz.*, S_{major}, S_{minor}, $\sigma_{\eta\eta}$ and R_9 [45–47]. For *DO*s and *BMO*s inside the ECAL, the aforementioned shower shape variables along with the ECAL timing information [45] can be utilised to distinguish such striking signatures and also to potentially reduce backgrounds. For signal signatures pertaining mostly to jets, let us discuss some possible shower-shape variables specifically for the HCAL.

- *BMOs:* This can happen if the LLP decays in one of the outer layers of the HCAL or even after crossing it and at least one decay product comes back to the HCAL. If the HCAL has depth-segmentation then the energy of each depth can be read-out separately. If $E(D_i)$ denotes the energy deposited in the i^{th} depth of a HCAL tower, then one can use $E(D_i)s$ as inputs to train a boosted decision tree (BDT) [48]. The BDT output should be a powerful discriminator between backward-moving signal jets and forward moving background jets.
- *DOs:* This situation can arise if the LLP decays before, inside or after the ECAL, and at least one decay product moves towards the HCAL. As already illustrated in figure 2, non-prompt jets can be asymmetric with respect to the HCAL towers. Let us assume that the largest fraction of energy of a jet is deposited in a tower, which is considered as the seed tower or 0^{th} tower. Then one can take the ratio of energy deposited in a 3×3 neighbourhood-plus-seed tower ($\sum_{i=0}^{8} E_i$) and the energy deposited in the seed tower (E_0) as presented in figure 2. For a prompt-jet depositing most of the energy in a single HCAL tower, this ratio is expected to be close to unity. However for non-prompt jets, depositing energy across several HCAL towers, the ratio should be less than unity. Thus, this variable can serve as a discriminator between distorted signal jets and prompt background jets. One can also construct S_{major} and S_{minor} variables for HCAL to exploit the elliptical signal jets in contrast to the circular background jets in $\eta - \phi$ plane. All these discriminating variables can be utilised to train a BDT, whose output should be a more powerful handle to reject backgrounds.

If an LLP decays just outside the muon detectors, then the *BMO*s are the only detectable objects in the signal. In such cases, the timing information of muon detectors (for example: resistive plate chambers in CMS) can be useful. If t_n is the timing of the hit in n^{th} layer of muon detector for a reconstructed muon-track, then $t_n < t_{n+1}$ will be the signature of outward-moving background tracks and $t_n > t_{n+1}$ will be the sign of a *BMO*. Here, the innermost layer is assumed to be the first layer and n increases as we move radially outwards. Something similar can not be done in silicon tracker, because of its slow response time.

Cosmic ray backgrounds can potentially mimic the *BMOs* [49]. One way to suppress such cosmic ray backgrounds is by tagging the LLP only in the lower half of the detector which will be free of any cosmic rays that move towards the beam-pipe.

In summary, we have sketched through several benchmarks, the importance to look for objects which ensue from a secondary vertex and are often at *large* angular separations with respect to the direction of the parent LLP. One of the main reasons to look for the *DOs* and the *BMOs* is that they can often be missed by standard searches. Besides, if the LLPs are typically heavier than 500 GeV, the production rates are small and hence yielding a small number of signal events. Thus, it is of utmost importance to be able to fully reconstruct the heavy LLPs through the energy-momenta in-

formation of all its visible decay products, in order to make quantitative statements about their mass, spin and CP-properties. For this simple analysis, we have only considered light jets as the visible objects. However, one can study other signatures involving leptons, photons or even boosted objects like top-jets, $W/Z/H$-jets. Besides, *DOs* and *BMOs* may help in the reduction of a significant portion of the backgrounds. Because of the complex nature of the signature, and the various possibilities depending on the lifetime of the LLP and its decay modes, the machine-learning techniques, aiming to achieve signal pattern recognition, can be of great help for such searches. These issues are left a future work.

Acknowledgments — We thank Nicolas Berger, Remi Lafaye, Sunanda Banerjee, Maurizio Pierini, Gustaaf H. Brooijmans and Giacomo Polesello for useful discussions. This work was supported in part by the French ANR project DMAstro-LHC (ANR-12-BS05-0006), by the *Investissements d'avenir* Labex ENIGMASS, by the Research Executive Agency of the European Union under the Grant Agreement PITN-GA2012-316704 (HiggsTools), by the CNRS LIA-THEP (Theoretical High Energy Physics) and the INFRE-HEPNET (IndoFrench Network on High Energy Physics) of CEFIPRA/IFCPAR (Indo-French Centre for the Promotion of Advanced Research). The work of SM is supported by the German Federal Ministry of Education and Research BMBF. The work of BB is supported by the Department of Science and Technology, Government of India, under the Grant Agreement number IFA13-PH-75 (INSPIRE Faculty Award). The work of RMG is supported by the Department of Science and Technology, India under Grant No. SR/S2/JCB-64/2007. BB acknowledges the hospitality of LAPTh where the major parts of this work was carried out. BB, SB, GB and FB acknowledge the Les Houches workshop series "Physics at TeV colliders" 2017 where the work was finalised.

* banerjee@lapth.cnrs.fr
† belanger@lapth.cnrs.fr
‡ biplob@chep.iisc.ernet.in
§ boudjema@lapth.cnrs.fr
¶ rohini@cts.iisc.ernet.in
** mukherjee@physik.rwth-aachen.de

[1] G. F. Giudice and R. Rattazzi, *Theories with gauge mediated supersymmetry breaking*, *Phys. Rept.* **322** (1999) 419–499, [hep-ph/9801271].

[2] A. Arvanitaki, N. Craig, S. Dimopoulos, and G. Villadoro, *Mini-Split*, *JHEP* **02** (2013) 126, [arXiv:1210.0555].

[3] Z. Chacko, H.-S. Goh, and R. Harnik, *The Twin Higgs: Natural electroweak breaking from mirror symmetry*, *Phys. Rev. Lett.* **96** (2006) 231802, [hep-ph/0506256].

[4] G. Burdman, Z. Chacko, H.-S. Goh, and R. Harnik, *Folded supersymmetry and the LEP paradox*, *JHEP* **02** (2007) 009, [hep-ph/0609152].

[5] R. T. Co, F. D'Eramo, L. J. Hall, and D. Pappadopulo, *Freeze-In Dark Matter with Displaced Signatures at Colliders*, *JCAP* **1512** (2015), no. 12 024, [arXiv:1506.07532].

[6] Y. Cui and B. Shuve, *Probing Baryogenesis with Displaced Vertices at the LHC*, *JHEP* **02** (2015) 049, [arXiv:1409.6729].

[7] **CMS** Collaboration, V. Khachatryan et al., *Search for Long-Lived Neutral Particles Decaying to Quark-Antiquark Pairs in Proton-Proton Collisions at $\sqrt{s} = 8$ TeV*, *Phys. Rev.* **D91** (2015), no. 1 012007, [arXiv:1411.6530].

[8] **ATLAS** Collaboration, G. Aad et al., *Search for massive, long-lived particles using multitrack displaced vertices or displaced lepton pairs in pp collisions at $\sqrt{s} = 8$ TeV with the ATLAS detector*, *Phys. Rev.* **D92** (2015), no. 7 072004, [arXiv:1504.05162].

[9] **LHCb** Collaboration, R. Aaij et al., *Search for long-lived particles decaying to jet pairs*, *Eur. Phys. J.* **C75** (2015), no. 4 152, [arXiv:1412.3021].

[10] **CMS** Collaboration, V. Khachatryan et al., *Search for long-lived particles that decay into final states containing two electrons or two muons in proton-proton collisions at $\sqrt{s} = 8$ TeV*, *Phys. Rev.* **D91** (2015), no. 5 052012, [arXiv:1411.6977].

[11] **CMS** Collaboration, V. Khachatryan et al., *Search for Displaced Supersymmetry in events with an electron and a muon with large impact parameters*, *Phys. Rev. Lett.* **114** (2015), no. 6 061801, [arXiv:1409.4789].

[12] **ATLAS** Collaboration, G. Aad et al., *Search for pair-produced long-lived neutral particles decaying in the ATLAS hadronic calorimeter in pp collisions at $\sqrt{s} = 8$ TeV*, *Phys. Lett.* **B743** (2015) 15–34, [arXiv:1501.04020].

[13] **ATLAS** Collaboration, G. Aad et al., *Search for long-lived neutral particles decaying into lepton jets in proton-proton collisions at $\sqrt{s} = 8$ TeV with the ATLAS detector*, *JHEP* **11** (2014) 088, [arXiv:1409.0746].

[14] **ATLAS** Collaboration, T. A. collaboration, *Search for long-lived neutral particles decaying into displaced lepton jets in proton–proton collisions at $\sqrt{s} = 13$ TeV with the ATLAS detector*, .

[15] P. Schwaller, D. Stolarski, and A. Weiler, *Emerging Jets*, *JHEP* **05** (2015) 059, [arXiv:1502.05409].

[16] **ATLAS** Collaboration, G. Aad et al., *Search for nonpointing and delayed photons in the diphoton and missing transverse momentum final state in 8 TeV pp collisions at the LHC using the ATLAS detector*, *Phys. Rev.* **D90** (2014), no. 11 112005, [arXiv:1409.5542].

[17] **CMS** Collaboration, V. Khachatryan et al., *Search for disappearing tracks in proton-proton*

collisions at $\sqrt{s} = 8$ *TeV*, *JHEP* **01** (2015) 096, [arXiv:1411.6006].

[18] S. Asai, Y. Azuma, M. Endo, K. Hamaguchi, and S. Iwamoto, *Stau Kinks at the LHC*, *JHEP* **12** (2011) 041, [arXiv:1103.1881].

[19] S. Jung and H.-S. Lee, *Constraining Higgsino Kink Tracks from Existing LHC Searches*, *Int. J. Mod. Phys.* **A32** (2017), no. 13 1750070, [arXiv:1503.00414].

[20] **ALEPH** Collaboration, R. Barate et al., *Search for gauge mediated SUSY breaking topologies at* $S^{(1/2)}$ *similar to 189-GeV*, *Eur. Phys. J.* **C16** (2000) 71–85.

[21] **ATLAS** Collaboration, G. Aad et al., *Search for displaced muonic lepton jets from light Higgs boson decay in proton-proton collisions at* $\sqrt{s} = 7$ *TeV with the ATLAS detector*, *Phys. Lett.* **B721** (2013) 32–50, [arXiv:1210.0435].

[22] N. Craig, A. Katz, M. Strassler, and R. Sundrum, *Naturalness in the Dark at the LHC*, *JHEP* **07** (2015) 105, [arXiv:1501.05310].

[23] D. Curtin and C. B. Verhaaren, *Discovering Uncolored Naturalness in Exotic Higgs Decays*, *JHEP* **12** (2015) 072, [arXiv:1506.06141].

[24] Z. Chacko, D. Curtin, and C. B. Verhaaren, *A Quirky Probe of Neutral Naturalness*, *Phys. Rev.* **D94** (2016), no. 1 011504, [arXiv:1512.05782].

[25] **CMS** Collaboration, V. Khachatryan et al., *Search for Decays of Stopped Long-Lived Particles Produced in Proton?Proton Collisions at* $\sqrt{s} = 8$ *TeV*, *Eur. Phys. J.* **C75** (2015), no. 4 151, [arXiv:1501.05603].

[26] **ATLAS** Collaboration, G. Aad et al., *Search for long-lived stopped R-hadrons decaying out-of-time with pp collisions using the ATLAS detector*, *Phys. Rev.* **D88** (2013), no. 11 112003, [arXiv:1310.6584].

[27] **D0** Collaboration, V. M. Abazov et al., *Search for stopped gluinos from* $p\bar{p}$ *collisions at* $\sqrt{s} =$ *1.96-TeV*, *Phys. Rev. Lett.* **99** (2007) 131801, [arXiv:0705.0306].

[28] **CMS Collaboration** Collaboration, *Search for heavy stable charged particles with* 12.9 fb^{-1} *of 2016 data*, Tech. Rep. CMS-PAS-EXO-16-036, CERN, Geneva, 2016.

[29] B. C. Allanach et al., *The Snowmass points and slopes: Benchmarks for SUSY searches*, *Eur. Phys. J.* **C25** (2002) 113–123, [hep-ph/0202233].

[30] L. Randall and R. Sundrum, *Out of this world supersymmetry breaking*, *Nucl. Phys.* **B557** (1999) 79–118, [hep-th/9810155].

[31] A. C. Kraan, *Interactions of heavy stable hadronizing particles*, *Eur. Phys. J.* **C37** (2004) 91–104, [hep-ex/0404001].

[32] R. Mackeprang and A. Rizzi, *Interactions of Coloured Heavy Stable Particles in Matter*, *Eur. Phys. J.* **C50** (2007) 353–362, [hep-ph/0612161].

[33] S. Dimopoulos, M. Dine, S. Raby, and S. D. Thomas, *Experimental signatures of low-energy gauge mediated supersymmetry breaking*, *Phys. Rev. Lett.* **76** (1996) 3494–3497, [hep-ph/9601367].

[34] P. W. Graham, D. E. Kaplan, S. Rajendran, and P. Saraswat, *Displaced Supersymmetry*, *JHEP* **07** (2012) 149, [arXiv:1204.6038].

[35] J. A. Evans and J. Shelton, *Long-Lived Staus and Displaced Leptons at the LHC*, *JHEP* **04** (2016) 056, [arXiv:1601.01326].

[36] M. J. Strassler and K. M. Zurek, *Discovering the Higgs through highly-displaced vertices*, *Phys. Lett.* **B661** (2008) 263–267, [hep-ph/0605193].

[37] T. Han, Z. Si, K. M. Zurek, and M. J. Strassler, *Phenomenology of hidden valleys at hadron colliders*, *JHEP* **07** (2008) 008, [arXiv:0712.2041].

[38] S. Banerjee, G. Bélanger, B. Mukhopadhyaya, and P. D. Serpico, *Signatures of sneutrino dark matter in an extension of the CMSSM*, *JHEP* **07** (2016) 095, [arXiv:1603.08834].

[39] Y. Bai and P. Schwaller, *Scale of dark QCD*, *Phys. Rev.* **D89** (2014), no. 6 063522, [arXiv:1306.4676].

[40] T. Sjostrand, S. Mrenna, and P. Z. Skands, *PYTHIA 6.4 Physics and Manual*, *JHEP* **05** (2006) 026, [hep-ph/0603175].

[41] **CMS** Collaboration, S. Chatrchyan et al., *Search for long-lived particles decaying to photons and missing energy in proton-proton collisions at* $\sqrt{s} = 7$ *TeV*, *Phys. Lett.* **B722** (2013) 273–294, [arXiv:1212.1838].

[42] **CMS** Collaboration, G. L. Bayatian et al., *CMS technical design report, volume II: Physics performance*, *J. Phys.* **G34** (2007), no. 6 995–1579.

[43] **CMS Collaboration** Collaboration, *Data Parking and Data Scouting at the CMS Experiment*, .

[44] Y. Gershtein, *CMS Hardware Track Trigger: New Opportunities for Long-Lived Particle Searches at the HL-LHC*, arXiv:1705.04321.

[45] **CMS Collaboration** Collaboration, *Search for long-lived neutral particles in the final state of delayed photons and missing energy in proton-proton collisions at* $\sqrt{s} = 8$ *TeV*, Tech. Rep. CMS-PAS-EXO-12-035, CERN, Geneva, 2015.

[46] **CMS** Collaboration, *Updated measurements of the Higgs boson at 125 GeV in the two photon decay channel*, .

[47] **CMS** Collaboration, V. Khachatryan et al., *Search for diphoton resonances in the mass range from 150 to 850 GeV in pp collisions at* $\sqrt{s} = 8$ *TeV*, *Phys. Lett.* **B750** (2015) 494–519, [arXiv:1506.02301].

[48] B. P. Roe, H.-J. Yang, J. Zhu, Y. Liu, I. Stancu, and G. McGregor, *Boosted decision trees, an alternative to artificial neural networks*, *Nucl. Instrum. Meth.* **A543** (2005), no. 2-3 577–584, [physics/0408124].

[49] **ATLAS** Collaboration, G. Aad et al., *Beam-induced and cosmic-ray backgrounds observed in the ATLAS detector during the LHC 2012 proton-proton running period*, *JINST* **11** (2016), no. 05 P05013, [arXiv:1603.09202].